**Title**

Investigating Ammonium By-product Removal for Ureolytic Bio-cementation Using Meter-scale Experiments

**Permalink**

https://escholarship.org/uc/item/8t96q183

**Journal**

Scientific Reports, 9(1)

**ISSN**

2045-2322

**Authors**

Lee, Minyong
Gomez, Michael G
San Pablo, Alexandra CM
et al.

**Publication Date**

2019

**DOI**

10.1038/s41598-019-54666-1

**Copyright Information**

Peer reviewed

OPEN

# Investigating Ammonium By-product Removal for Ureolytic Bio-cementation Using Meter-scale Experiments

Minyong Lee [1], Michael G. Gomez [1]*, Alexandra C. M. San Pablo [2], Colin M. Kolbus [1], Charles M. R. Graddy [3], Jason T. DeJong [2] & Douglas C. Nelson [3]
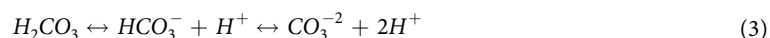
Microbially Induced Calcite Precipitation (MICP), or bio-cementation, is a promising bio-mediated technology that can improve the engineering properties of soils through the precipitation of calcium carbonate. Despite significant advances in the technology, concerns regarding the fate of produced $NH_4^+$ by-products have remained largely unaddressed. In this study, five 3.7-meter long soil columns each containing one of three different soils were improved using ureolytic bio-cementation, and post-treatment $NH_4^+$ by-product removal was investigated during the application of 525 L of a high pH and high ionic strength rinse solution. During rinsing, reductions in aqueous $NH_4^+$ were observed in all columns from initial concentrations between $\approx$100 mM to 500 mM to final values between $\approx$0.3 mM and 20 mM with higher $NH_4^+$ concentrations observed at distances furthest from the injection well. In addition, soil $V_s$ measurements completed during rinse injections suggested that no significant changes in cementation integrity occurred during $NH_4^+$ removal. After rinsing and a 12 hour stop flow period, all column solutions achieved cumulative $NH_4^+$ removals exceeding 97.9%. Soil samples collected following rinsing, however, contained significant sorbed $NH_4^+$ masses that appeared to have a near linear relationship with surrounding aqueous $NH_4^+$ concentrations. While these results suggest that $NH_4^+$ can be successfully removed from bio-cemented soils, acceptable limits for $NH_4^+$ aqueous concentrations and sorbed $NH_4^+$ masses will likely be governed by site-specific requirements and may require further investigation and refinement of the developed techniques.

Microbially Induced Calcite Precipitation (MICP), or bio-cementation, has shown significant promise as an environmentally-conscious alternative to geotechnical ground improvement technologies, which have traditionally relied upon hazardous grouting chemicals, high mechanical energy, and energy-intensive materials to improve the engineering properties of soils[1–3]. In the urea hydrolysis (ureolysis) driven process, microorganisms containing urease enzymes are used to catalyze a reaction that degrades urea, yielding total ammonium ($NH_4^+$), dissolved inorganic carbon, and hydroxide ions[4] [Eqs. (1–3)]. When soluble calcium is available from either treatment solutions or groundwater, resulting alkalinity can supersaturate solutions with respect to calcium carbonate ($CaCO_3$) and initiate mineral precipitation on soil particle surfaces and contacts [Eq. (4)]. Resulting bio-cementation can improve the engineering properties of soils through large increases in shear stiffness and strength with small reductions in hydraulic conductivity and porosity[5–8]. The process has been proposed for a variety of applications including mitigation of earthquake-induced soil liquefaction, general geotechnical soil improvement, subsurface flow manipulation, and divalent contaminant immobilization among other uses[1,9–12].

$$(NH_2)_2CO + 2H_2O \rightarrow 2NH_3 + H_2CO_3 \qquad (1)$$

$$NH_3 + H_2O \leftrightarrow NH_4^+ + OH^- \qquad (2)$$
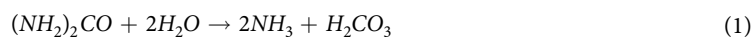
[1]Department of Civil and Environmental Engineering, University of Washington, Seattle, WA, 98195, USA. [2]Department of Civil and Environmental Engineering, University of California, Davis, CA, 95616, USA. [3]Department of Microbiology and Molecular Genetics, University of California, Davis, CA, 95616, USA. *email: mggomez@uw.edu

$$H_2CO_3 \leftrightarrow HCO_3^- + H^+ \leftrightarrow CO_3^{-2} + 2H^+ \qquad (3)$$

$$Ca^{+2} + CO_3^{-2} \leftrightarrow CaCO_{3(solid)} \qquad (4)$$

Researchers have made significant advances in the technology in recent years, including identifying alternative treatment techniques[13,14], up-scaling the process to meter-scale[15–19], and characterizing the engineering behavior of bio-cemented soils[8,20]. Despite these advances, environmental concerns regarding the fate of produced $NH_4^+$ by-products have remained largely unaddressed[1,21]. $NH_4^+$ is a commonly encountered source of inorganic nitrogen in soil systems, however, high aqueous $NH_4^+$ concentrations produced following ureolytic MICP may present serious environmental and human health concerns if left untreated in soils and groundwater. For example, the presence of high $NH_4^+$ in surface waters can encourage the growth of toxic algal blooms, which can decrease aquatic dissolved oxygen availability, produce high levels of toxins, and encourage bacterial growth, therefore threatening fish, humans, and other flora and fauna[22]. While no maximum contaminant level has been established by the U.S. EPA for total $NH_4^+$ in drinking water, maximum concentrations for aquatic life of 17 mg/L ($\approx$1 mM) and 1.9 mg/L ($\approx$0.1 mM) total $NH_4^+$ for acute and chronic exposure, respectively, have been recommended[23]. During field-scale applications, aqueous $NH_4^+$ concentrations produced during bio-cementation will likely require removal to meet water quality standards and or maintain similar water quality as that present prior to treatments. $NH_4^+$ concentrations near twice the concentration of applied urea are expected by reaction stoichiometry [Eq. (1)], with many past experiments resulting in the production of $NH_4^+$ concentrations exceeding 500 mM. Limited understanding of post-treatment $NH_4^+$ removal has been a significant barrier for bio-cementation technology that has limited field-scale applications and environmental benefits. In order for MICP to be a truly environmentally beneficial technology, methods to manage, remediate, or remove $NH_4^+$ by-products following bio-cementation are needed.

While in-situ nitrification of produced $NH_4^+$ to nitrite ($NO_2^-$) and nitrate ($NO_3^-$) (under aerobic conditions) and subsequent denitrification of $NO_3^-$ to nitrogen gases (under anaerobic conditions) may offer a potential remediation strategy, these processes will be challenging and likely unpractical at field-scale due to the need for dramatic modifications in subsurface oxygen availability and chemical conditions. In addition, Gat et al.[21] showed that in-situ oxidation of $NH_4^+$ can have detrimental effects on bio-cementation integrity resulting from the generation of acidity in this process, further suggesting the need to address produced $NH_4^+$ following bio-cementation. Although few studies have examined and quantified the removal of $NH_4^+$ by-products following MICP, "rinse" solutions have been most commonly applied to remove $NH_4^+$ from treated areas with subsequent remediation of collected effluent completed ex-situ at water reclamation facilities[15,24]. Post-treatment rinsing may require significant energy and materials when applied at field scale, however, the technique can provide an effective strategy for $NH_4^+$ management following bio-cementation in the absence of other remediation processes and may provide an opportunity for $NH_4^+$ recovery. Recently, centimeter-scale soil column experiments were performed to further investigate and quantify the removal of $NH_4^+$ by-products following MICP in a clean poorly-graded Concrete Sand material using rinse solution injections[25]. Results suggested that removal of positively-charged $NH_4^+$ ions from clean sands may be significantly more difficult due to interactions with negatively-charged soil particle surfaces. When rinse solutions of differing ionic strength and pH were applied, $NH_4^+$ removal was improved with increases in ionic strength, while pH had no detectable influence on removal. Improved removal was attributed to the exchange of $NH_4^+$ existing on soil surfaces with $Ca^{2+}$ cations supplied from rinse solutions. A high pH (pH = 9.0) and high ionic strength (500 mM $CaCl_2$) rinse solution was identified that improved $NH_4^+$ removal while simultaneously limiting dissolution of bio-cementation. Although these results were promising, it remained unclear if these techniques would remain effective at meter-scale treatment distances.

In this study, five 3.7-meter long soil columns were improved using ureolytic bio-cementation, and post-treatment $NH_4^+$ by-product removal was investigated as a function of different soil materials and treatment techniques. Columns contained three different poorly-graded sand materials including: an alluvial sand (Column 1, 2, and 3), a marine sand (Column 4), and a second alluvial sand material (Column 5). Prior to bio-cementation, all columns received different biological treatments over the first six days intended to either enrich native ureolytic microorganisms or augment Sporosarcina pasteurii (S. pasteurii) bacteria uniformly across column lengths. Three different biological treatment strategies were applied to enrich native ureolytic microorganisms to achieve high (Column 1) and low bulk ureolytic rates (Column 2, 4, 5) and augment soils with S. pasteurii at a high cell density (Column 3) to obtain a high ureolytic rate similar to Column 1. Differences in achieved ureolytic rates were intended to examine the effect of urea hydrolysis rate on the spatial uniformity and extent of bio-cementation; the results of which are more extensively described in a separate manuscript[26]. Following biological treatments, nine cementation injections containing identical calcium and urea concentrations were applied to all columns over nine (Column 1, 3) and eighteen (Column 2, 4, 5) days. All columns achieved differing degrees of bio-cementation with distance from the injection well. Following MICP treatments, 525 L of a high pH and high ionic strength rinse solution was applied to each column to remove produced $NH_4^+$. During rinse injections, changes in $NH_4^+$ by-product removal and effects on bio-cementation integrity were monitored. Following rinsing, physical soil samples were collected at various locations and sorbed $NH_4^+$ masses remaining on soil surfaces were quantified.

| Soil Material | USCS | Deposition | $D_{10}$ (mm) | $D_{30}$ (mm) | $D_{60}$ (mm) | Fines Content (%) | $e_{min}$ | $e_{max}$ |
|---|---|---|---|---|---|---|---|---|
| Concrete Sand | SP | Alluvial | 0.23 | 0.54 | 1.54 | 1.1 | 0.35 | 0.60 |
| Delta Sand | SP | Marine | 0.19 | 0.25 | 0.37 | 1.3 | 0.48 | 0.95 |
| Covelo Sand | SP | Alluvial | 0.23 | 0.52 | 1.55 | 1.6 | 0.38 | 0.59 |
| Monterey Sand | SP | Marine | 1.01 | 1.15 | 1.45 | 0 | — | — |

**Table 1.** Summary of Soil Properties.

| Column No. | Experimental Measurements | | | | PHREEQC Model Parameters | |
|---|---|---|---|---|---|---|
| | Soil Material | Porosity | Relative Density (%) | Total Pore Volume (L) | Porosity | Longitudinal Dispersivity (m) |
| 1 | Concrete Sand | 0.31 | 56 | 50.7 | 0.23 | 0.3 |
| 2 | Concrete Sand | 0.30 | 67 | 48.5 | 0.23 | 0.3 |
| 3 | Concrete Sand | 0.32 | 56 | 50.6 | 0.25 | 1.5 |
| 4 | Delta Sand | 0.40 | 58 | 63.0 | 0.33 | 0.1 |
| 5 | Covelo Sand | 0.32 | 55 | 50.3 | 0.25 | 1.5 |

**Table 2.** Summary of Soil Column Properties and PHREEQC Model Parameters.

## Materials and Methods

**Soil materials.** Four different clean poorly-graded sands were used to prepare soil columns. Column 1, 2, and 3 contained the same alluvial Concrete Sand used in past experiments[18,25,27,28], Column 4 contained a marine Delta Sand, and Column 5 contained an alluvial Covelo Sand. In all columns, coarser Monterey Sand was placed at column ends as a filter material. Soil properties including USCS classification following ASTM D2487-10[29], depositional environment, $D_{10}$, $D_{30}$, $D_{60}$, fines content (% <#200 sieve), and minimum ($e_{min}$) and maximum ($e_{max}$) void ratios are summarized for all sands in Table 1.

**Soil columns.** Five 3.7-meter long hollow steel columns with square cross-sections (0.2 m by 0.2 m) contained 0.15 $m^3$ of sand and received treatment injections in one direction to simulate a single stream tube within a well-to-well half-space. Treatment wells (ID = 26.6 mm) were located on column ends and had valves, which allowed for pressurization of the injection well and removal of effluent solutions at the outlet well. Soils were placed in three ≈16 to 76 mm lifts, which allowed for bender element sensors to be placed at mid-height within columns during soil placement. Lifts were moist tamped and surfaces were scarified to limit density differences between lifts. Table 2 summarizes soil material types, soil column porosities, relative densities, and pore volumes determined from placed soil masses. In all columns, estimated porosities were between 0.30 and 0.40, relative densities were between 55% and 67%, and column pore volumes (PV) varied between 48.5 L and 63.0 L. Columns contained four bender element sensor pairs at distances of 0.31 m, 1.33 m, 2.35 m, and 3.37 meters from the injection location to monitor changes in soil shear wave velocities ($V_s$), indicative of bio-cementation. Four aqueous sampling ports were placed at distances of 0.15 m, 0.83 m, 1.82 m, and 2.81 m away from the injection location to monitor injection pressures and obtain solution samples at various times. Sampling ports consisted of 0.15 m long steel tubes (ID = 3.35 mm) with 25.4 mm diameter circular plastic filters (125–195 μm) open at mid-height within columns. A fifth drain port, consisting of a 60.3 mm ball valve with a porous filter material, was used to obtain additional samples and was located 3.58 m away from the injection location at the bottom of columns. Figure 1 provides a detailed schematic and images of soil columns including treatment application systems, bender element and sampling port locations, and treatment wells.

**Saturation and bromide passive tracer testing.** Prior to all treatments, columns were slowly saturated with an artificial ground water (AGW) solution containing 40 μM $KNO_3$, 450 μM $MgSO_4$, 1.75 mM $CaCl_2$, 40 μM $NaNO_3$, 1.1 mM $NaHCO_3$, and 60 μM $KHCO_3$ following Ferris et al.[30]. Immediately following saturation and before all bio-cementation treatments, columns received passive tracer injections to evaluate differences in solution transport between columns. During tracer testing, 76 L of a 15 mM NaBr solution was injected, followed by 76 L of de-ionized water to examine the arrival and removal of passive $Br^-$ ions at the outlet well. A constant flow rate of 400 mL/min was used for injections and solution samples were collected at outlet wells once every 5 minutes. Solution conductivities were measured and normalized by the conductivity of the injected NaBr solution to estimate normalized $Br^-$ concentrations ($C/C_0$). One-dimensional advective-dispersive soil column transport models were developed using the geochemical software PHREEQC[31] and were used to match passive tracer experimental observations by varying porosities and longitudinal dispersivities for all columns. All models were composed of 42 cells (0.089 meters each) and received NaBr and de-ionized water injections that were identical to the physical experiment.

**Treatment injections.** Following passive tracer testing, all columns received different treatment solutions in a series of three treatment phases: (1) enrichment/augmentation, (2) cementation, and (3) $NH_4^+$ rinsing. Table 3 presents a summary of treatment schemes including solution chemical constituents and concentrations, injection numbers and volumes, and injection and stop flow time durations for all columns. In the first treatment phase,
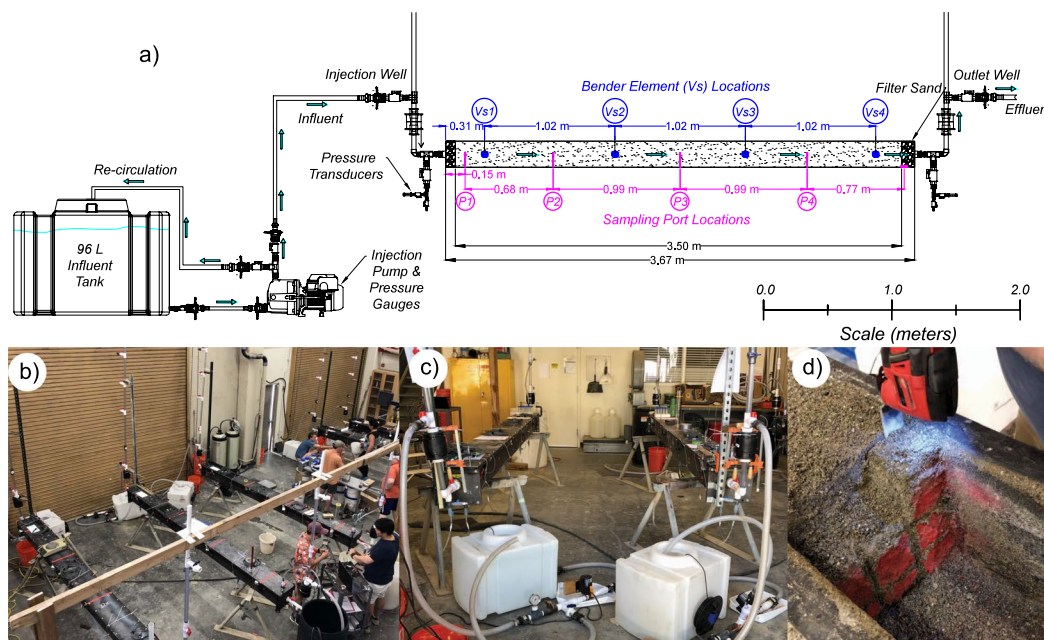
**Figure 1.** Overview of meter-scale experiments including: (**a**) schematic of meter-scale soil columns with treatment application systems, sampling ports, and bender element locations, (**b**) images of soil columns during treatments, (**c**) treatment solution injection systems, and (**d**) bio-cemented soil materials during post-rinsing soil sampling.

| Solution Constituent | Column 1 | | Column 2, 4, & 5 | | Column 3 | | All Columns |
|---|---|---|---|---|---|---|---|
| | Enrichment | Cementation | Enrichment | Cementation | Augmentation | Cementation | NH$_4^+$ Rinsing |
| Calcium Chloride (mM) | — | 250 | — | 250 | — | 250 | 200 |
| Urea (mM) | 50 | 250 | 50 | 250 | — | 250 | — |
| Ammonium Chloride (mM) | 100 | 12.5 | 100 | 12.5 | — | 12.5 | — |
| Sodium Acetate (mM) | 42.5 | 42.5 | 42.5 | 42.5 | — | 42.5 | — |
| Yeast Extract (g/L) | 0.2 | 0.2 | 0.04 | 0.02 | — | — | — |
| Sodium Hydroxide (g/L) | 1.28 | — | 1.28 | — | — | — | — |
| NaCl (g/L) | — | — | — | — | 9 | — | — |
| S. pasteurii (cells/mL) | — | — | — | — | $9.36 \times 10^7$* $1.40 \times 10^6$** | — | — |
| Initial Solution pH | 9.0 | 8.4 | 9.0 | 8.4 | ≈7.0 | 8.4 | 10.0 |
| Number of Injections | 6 | 9 | 6 | 9 | 2 | 9 | 1 |
| Injection Volume (L) | 76 | 76 | 76 | 76 | 76* 456** | 76 | 525 |
| Injection Duration (min) | 186 | 186 | 186 | 186 | 186* 1,140** | 186 | 700 |
| Stop Flow Period (hours) | 20.8 | 20.8 | 20.8 | 44.8 | 24.5 | 20.8 | 12.3 |

**Table 3.** Summary of Solution Constituents and Injection Schemes for All Columns. *First augmentation treatment. **Second augmentation treatment.

solutions were applied to either enrich soil columns for native ureolytic microorganisms (Column 1, 2, 4, 5) or augment soils with the highly active ureolytic bacterium, *S. pasteurii* (Column 3). Enriched columns received six enrichment treatments once daily with varying concentrations of yeast extract intended to achieve different ureolytic activities. Column 1 received higher yeast extract concentrations (0.2 g/L) following past experiments[14]

wherein high ureolytic activities were targeted (hydrolysis of 250 mM urea within ≈8 hours). Columns 2, 4, and 5 received lower yeast extract concentrations (0.04 g/L) to obtain a low bulk ureolytic rate (hydrolysis of 250 mM urea within ≈48 hours). Column 3 was inoculated on the last day of enrichment treatments by injecting 76 L of an isotonic saline solution (9 g/L NaCl) containing *S. pasteurii* (ATCC strain 11859) at a cell density of $9.36 \times 10^7$ cells/mL, intended to match the high ureolytic rate of Column 1. Due to lower ureolytic activity than expected along Column 3, a second augmentation injection consisting of 456 L of isotonic saline with $1.4 \times 10^6$ cells/mL was applied after the fourth cementation injection. Following all enrichment treatments, a flush solution that was identical to cementation solutions, but did not contain urea and $Ca^{2+}$, was applied to all enriched columns immediately before the first cementation treatment to remove high aqueous carbonate species expected after enrichment. Cementation treatments containing $Ca^{2+}$ were then applied to all columns to initiate $CaCO_3$ precipitation for a total of nine injections. Columns 1 and 3 received cementation treatments once every 24 hours and Columns 2, 4, and 5 received treatments once every 48 hours to allow near full hydrolysis to occur. During enrichment, augmentation, and cementation treatments, injection volumes of 76 L were applied at a constant flow rate of 400 mL/min, during which injected solutions were continuously mixed within injection tanks. Following cementation treatments, a 200 mM $CaCl_2$ solution (initial pH ≈ 10.0) was applied to all columns to remove $NH_4^+$ following previously identified strategies[25]. During $NH_4^+$ by-product removal injections, a rinse solution volume of 525 L was injected into each column at a flow rate of 750 mL/min and lasted ≈700 minutes. Following rinse injections, columns remained saturated for 12 hours during a stop flow period until columns were disassembled. All solutions were injected using small pumps (Wayne Inc., 0.1 HP) with pressure gauges to monitor injection pressures.

**Aqueous sampling.** Before and immediately after treatment injections, aqueous samples of ≈10 mL were collected from all sampling ports. On select days, aqueous samples were also collected 1, 2, 4, and 8 hours after injections to monitor ureolytic activity and chemical changes in time. Prior to all sample collection events, 30 mL of solution was removed from ports and discarded to obtain representative samples. During $NH_4^+$ rinse injections, ≈10 mL samples were collected from outlet wells once every 20 minutes and from all sampling ports and well locations once every 60 minutes. Aqueous samples were immediately frozen and stored at −20 °C until subsequent chemical analyses.

**Shear wave velocity measurements.** Shear wave velocity ($V_s$) measurements were obtained using horizontally-oriented bender element sensor pairs placed at mid-depth within columns at various distances from the injection well. $V_s$ measurements were obtained at all locations before and immediately after all biological and cementation injections. Additional measurements were performed during $NH_4^+$ rinsing before, 120, 240, 480, and 700 minutes after the start of rinse injections and following a 12-hour stop flow period (24 hours after start of rinse injections). Bender elements were coated with epoxy, electronics wax, and an insulating coating to waterproof sensors following similar processes detailed in Gomez et al.[18]. Transmitting bender elements were excited with a 24 V 100 Hz square wave and signals from receiving bender elements were measured and recorded using an oscilloscope at a sampling frequency of 1 MHz. Shear wave arrival times were interpreted visually and $V_s$ values were calculated from measured sensor spacings.

**Aqueous measurements.** Solution pH measurements were completed using a semi-micro pH electrode and meter system that was calibrated daily using a three-point buffer sequence (4.01, 7.00, 10.00) and had ± 0.01 pH unit accuracy. Total $NH_4^+$ measurements were completed using a salicylate reaction method similar to Krom (1980)[32], wherein two reagents (Reagent A & B) were added to dilute sample volumes and absorbance values were measured at 650 nm using a microplate spectrophotometer. Reagent A consisted of 1.9 mM sodium nitroprusside, 811 mM sodium salicylate, 387 mM sodium citrate, and 515 mM sodium tartrate in water. Reagent B consisted of 1.32 mM sodium hypochlorite and 1.5 M sodium hydroxide in water. Urea measurements were completed using a colorimetric urea assay similar to Knorst et al.[33]. A colorimetric reagent consisting of 216 mM p-dimethylaminobenzaldehyde, 2.32 M hydrochloric acid, and 13.83 M ethanol in water was added to dilute samples and absorbance values were measured at 422 nm using a microplate spectrophotometer. Conductivity measurements were completed using a conductivity probe and meter. Augmented cell densities were determined through direct counting[34].

**Cation exchange capacity and exchangeable cation measurements.** Cation exchange capacity (CEC) and exchangeable cation measurements were completed for untreated sand materials using a process similar to U.S. EPA Method 9080[35]. Soil CEC values reflect the capacity of negatively-charged soil surfaces to bind positively-charged ions, thus it was hypothesized that CEC differences between soils could influence $NH_4^+$ transport and removal following bio-cementation. During these measurements, 10 grams of untreated dry soil and 50 mL of a 1 M $NH_4Cl$ solution were added to a plastic syringe. After a 12-hour residence period, soil solutions were extracted, collected, and select exchangeable cations were characterized using inductively coupled plasma mass spectrometry (ICP-MS). Remaining extracted soil samples were then rinsed with ethanol for 6 hours to remove $NH_4^+$ ions that may have remained in free solution. Finally, 50 mL of 1 M KCl solution was added to all samples and allowed to equilibrate for 12 hours to encourage replacement of sorbed $NH_4^+$. Soil solutions were then extracted again and $NH_4^+$ concentrations in the extracted solution were quantified using the salicylate colorimetric assay. Measured $NH_4^+$ concentrations were used to calculate soil CEC values.

**Soil sampling and soil $NH_4^+$ measurements.** Following all treatments, column top caps were removed, and soil samples were collected at various locations at the center of columns. At heavily cemented locations, soil samples required removal using an oscillating power saw (Fig. 1d). Following sample collection, moist soil samples were frozen and stored at −20 °C until subsequent chemical analyses could be completed. An extraction process was used to quantify $NH_4^+$ masses remaining within soil samples. Free soil solution was first removed

| Sand | CEC (meq per 100 g soil) | Exchangeable Cations (µg per gram of soil) | | | | | | | | | |
|---|---|---|---|---|---|---|---|---|---|---|---|
| | | $Al^{3+}$ | $Ba^{2+}$ | $Ca^{2+}$ | $K^+$ | $Mg^{2+}$ | $Mn^{2+}$ | $Na^+$ | $S^{2+}$ | $Si^{4+}$ | $Zn^{2+}$ |
| Concrete Sand | 2.58 | <0.1 | 21.4 | 277.7 | 18.9 | 191.5 | <0.1 | 23.9 | 3.6 | 9.9 | <0.1 |
| Delta Sand | 4.32 | <0.1 | 13.5 | 236.7 | 84.0 | 238.8 | 1.5 | 180.1 | 81.8 | 9.6 | <0.1 |
| Covelo Sand | 1.64 | 0.7 | 9.4 | 555.3 | 18.7 | 59.6 | 1.3 | 5.7 | 17.0 | 4.8 | 2.3 |
| Concrete Sand w/10% $CaCO_3$ | 2.52 | <0.1 | 14.8 | 910.1 | 16.7 | 129.5 | <0.1 | 17.8 | 3.7 | 6.7 | <0.1 |

**Table 4.** Summary of Cation Exchange Capacity and Exchangeable Cation Analyses for Sands.

from thawed moist soil samples using a centrifuge process wherein 30 grams of moist soil samples (of known water content) were added to conical centrifuge tubes with 0.45 micron nylon filter baskets and centrifuged at 4150 rpm for 20 minutes to extract solutions. A minimum volume of 2 mL was collected, frozen, and stored at −20 °C until $NH_4^+$ concentrations were analyzed. Sorbed $NH_4^+$ masses remaining on soil particle surfaces were quantified using a KCl extraction process following Keeney & Nelson (1982)[36]. In this process, 10 gram moist soil samples (of known water content) were mixed with 20 mL of a 2 M KCl solution and allowed to equilibrate for at least 4 hours to facilitate removal of $NH_4^+$ ions. Soil solution mixtures were then added to another conical filter tube, centrifuged, and a 2 mL solution sample was collected, frozen, and stored at −20 °C until $NH_4^+$ concentrations were analyzed. KCl extracted $NH_4^+$ measurements included $NH_4^+$ initially present in free soil solutions as well as $NH_4^+$ masses that were initially sorbed to soil surfaces. Sorbed $NH_4^+$ masses were therefore estimated by subtracting $NH_4^+$ masses expected from free solution from $NH_4^+$ measurements following KCl extraction. Sorbed $NH_4^+$ masses were normalized per gram of dry soil.

**Statement on consent to publish.** The authors have notified persons shown in Fig. 1 and have received consent to publish images.

## Results and Discussion

Results from soil CEC and exchangeable cation measurements are summarized below in Table 4 for all three sands. A fourth sample consisting of Concrete Sand augmented with 10% by mass reagent-grade $CaCO_3$ was also tested to assess the potential influence of $CaCO_3$ minerals on soil CEC. As shown, Delta Sand had the highest CEC (4.32 meq/100 g) with Covelo Sand exhibiting the lowest CEC of tested sands (1.64 meq/100 g). Additionally, when $CaCO_3$ was added to the Concrete Sand sample, no significant effects on CEC were observed suggesting that the presence of bio-cementation $CaCO_3$ minerals likely had little influence on the ability of soils to bind $NH_4^+$ ions. When examining exchangeable cation concentrations, sands generally had similar values for common soil cations. Delta Sand, however, had notably higher $K^+$, $Mg^{2+}$, $Na^+$, and $S^{2+}$ concentrations than other tested sands, which was consistent with the marine depositional environment from which it was obtained. Exchangeable cations in Concrete Sand and Covelo Sand were most similar, however, Covelo Sand had significantly higher $Al^{3+}$ and $Ca^{2+}$ concentrations as well as much lower $Mg^{2+}$ concentrations than other sands. While tested sands had minor CEC and exchangeable cation differences, values were generally consistent with those expected for clean quartz sands[37].

Figure 2 presents measurements of normalized solution conductivity ($C/C_0$) versus injected NaBr tracer solution volume from samples obtained at outlet wells during passive tracer testing. Differences in $C/C_0$ values with injected volume are reflective of porous media advective-dispersive transport properties including porosity, hydrodynamic dispersion, and diffusion[38]. Immediately after starting the 15 mM NaBr solution injection, most $C/C_0$ values were near zero with small values (<10% $C/C_0$) observed exiting columns due to background soil solution conductivities. In Column 4, containing Delta Sand, notably larger initial $C/C_0$ values were observed and were consistent with the higher exchangeable cations measured previously (Table 4). After additional tracer solution was injected, $C/C_0$ values increased above background levels ($C/C_0 \approx 20\%$) in Column 1, 2, 3, and 5 after injecting ≈20 to 30 L (0.39 to 0.62 PV). Column 4 had a much more delayed arrival, however, with $C/C_0$ values increasing above ≈20% only after ≈42 L (0.66 PV). The delayed breakthrough in Column 4 was consistent with the higher porosity measured in this column (Table 2). After injecting the 76 L volume, $C/C_0$ values measured at the outlet well were between 94% and 96% for Column 1 and 2, 89% and 90% for Column 3 and 5, and were 98% for Column 4. While it was expected that Column 1, 2, and 3, which all contained Concrete Sand, would have similar breakthrough curves, the Column 3 breakthrough was distinctly different. Column 3 and 5, however, were found to have very similar breakthrough curve behaviors despite containing different sands. While unexpected, both Concrete Sand and Covelo Sand had similar grain size distributions and differences in transport properties may have resulted from differences in soil preparation between columns and minor preferential flow at the column boundaries. To better quantify transport differences between columns one-dimensional advective-dispersive soil column transport models were calibrated to match experimental trends by varying column longitudinal dispersivities ($\alpha$) and porosities (n). Modelled results are presented in Fig. 2 and porosity and dispersivity values used for models are summarized in Table 2. Modelled porosities were lower than those calculated from soil mass measurements for all columns, likely due to incomplete saturation, which could have reduced the apparent porosity of columns. When comparing dispersivity values between columns, a large increase in longitudinal dispersivities was observed between Column 1 and 2 ($\alpha = 0.3$ m) and Column 3 and 5 ($\alpha = 1.5$ m), despite having similar porosities. Column 4 had a similar dispersivity ($\alpha = 0.1$ m) as Column 1 and 2, but a much larger modeled porosity ($n_{model} = 0.33$) as expected from soil mass measurements.
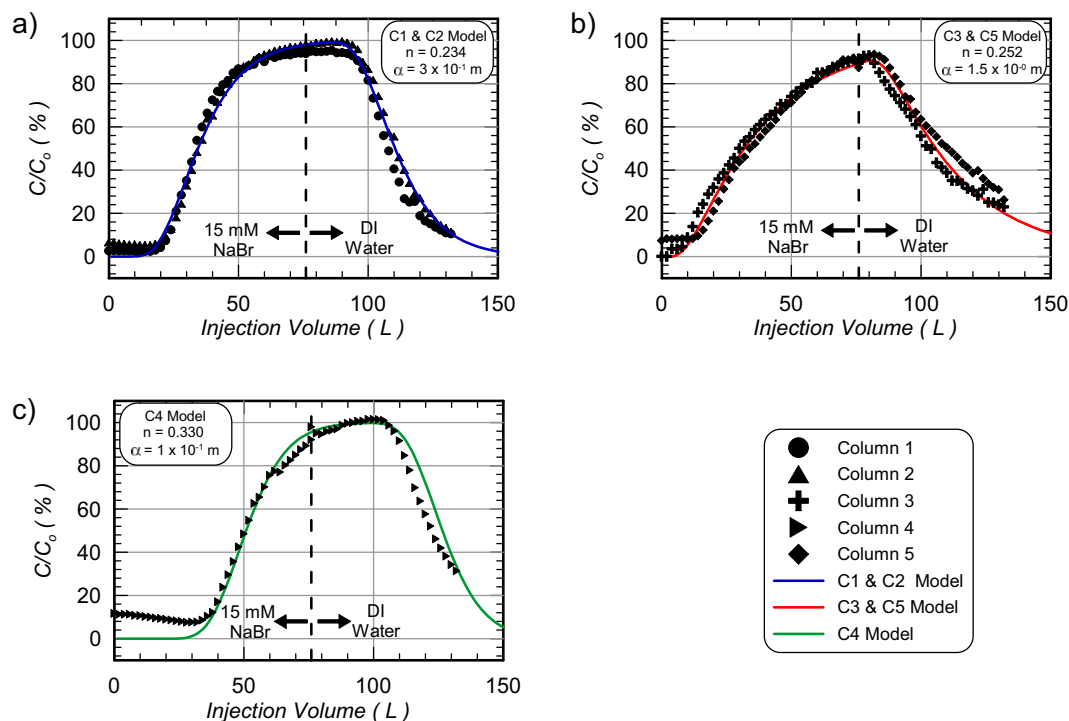
**Figure 2.** Measurements of normalized bromide concentrations ($C/C_0$) versus injected volume during passive tracer testing for (**a**) Column 1 and 2, (**b**) Column 3 and 5, and (**c**) Column 4 with PHREEQC modelled comparisons.
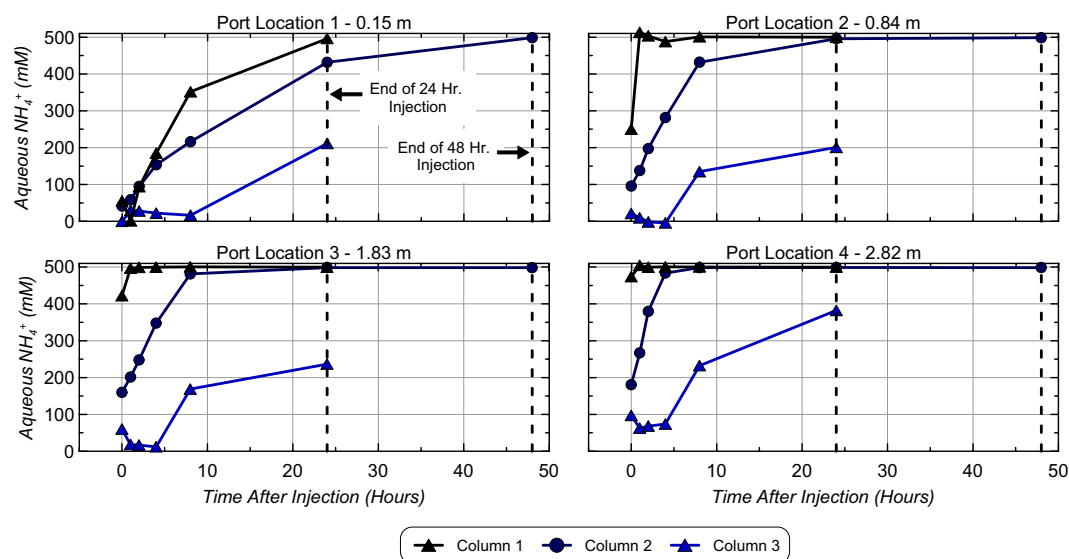


**Figure 3.** Changes in aqueous $NH_4+$ concentrations in time at all aqueous sampling port locations during the ninth cementation treatment.

Figure 3 presents aqueous $NH_4^+$ concentrations in time following the ninth cementation injection for Column 1, 2, and 3 from measurements at all port locations, immediately after injections, and 1, 2, 4, 8, 24, and 48 hours (when applicable) after injections. Aqueous $NH_4^+$ concentrations were determined by difference and reaction stoichiometry from direct urea measurements in time. While similar data were also obtained for Column 4 and 5, only Column 2 data are shown and was representative of trends observed in all enriched low ureolysis rate columns (Column 2, 4, 5). As shown, similar $NH_4^+$ production trends in time were observed between columns at each port location. Immediately after injections, aqueous $NH_4^+$ concentrations were lowest at the 0.15 m port location and increased with distance from the injection well for all columns due to urea hydrolysis occurring during solution transport as well as mixing with previously reacted solutions. At a distance of 0.15 m in the high
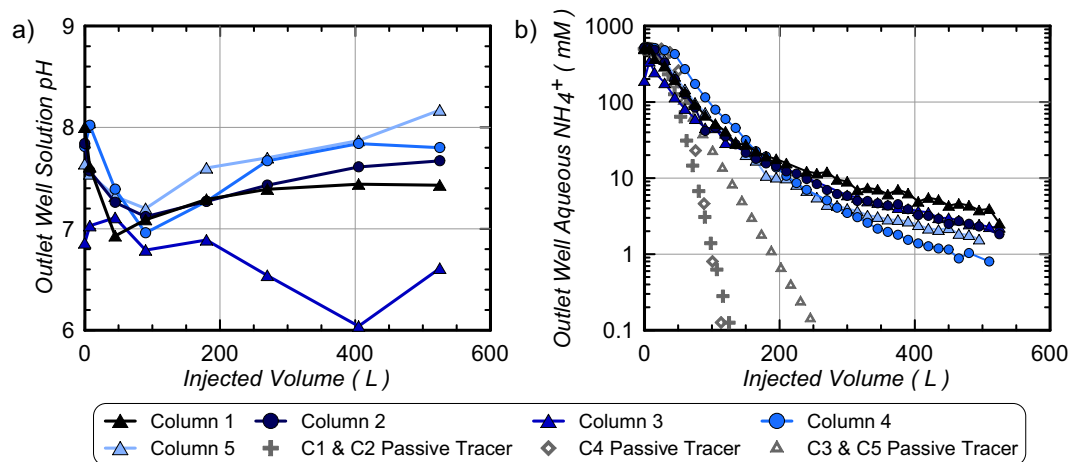
**Figure 4.** Measurements of outlet well (**a**) solution pH and (**b**) aqueous $NH_4^+$ concentrations versus injected rinse solution volume with PHREEQC modeled passive tracer comparisons.

ureolysis rate Column 1, $NH_4^+$ concentrations increased from post-treatment values near $\approx 50$ mM to $\approx 500$ mM over 24 hours, while $\approx 500$ mM concentrations were achieved at all other ports within 1 hour after injections. In the low ureolysis rate Column 2, $NH_4^+$ concentrations increased from post-treatment values near $\approx 50$ mM to $\approx 500$ mM at a distance of 0.15 m within 48 hours, and to $\approx 500$ mM at all other ports between 6 and 24 hours after injections. In the augmented Column 3, a slower rate of urea hydrolysis was consistently observed at all port locations relative to enriched columns. This resulted in significantly lower $NH_4^+$ concentrations between $\approx 200$ mM and $\approx 400$ mM residing after 24 hour treatment periods and a significant fraction of injected urea remaining non-hydrolyzed due to low ureolytic activity. Localization of ureolytic activity near injection well locations has been previously observed in augmented experiments[39] and likely resulted from the colloidal filtration of *S. pasteurii* bacterial cells during augmentation of Column 3[40]. Despite much lower $NH_4^+$ production observed in Column 3, all enriched columns (1, 2, 4, 5) achieved similar post-treatment $NH_4^+$ concentrations near $\approx 500$ mM after 24 hour (Column 1) and 48 hour residence periods (Columns 2, 4, 5).

Figure 4 presents solution pH and aqueous $NH_4^+$ concentration measurements for outlet well samples versus injected rinse solution volume. As shown in Fig. 4a, solutions initially exiting all enriched columns had pH values between 7.6 and 8.0. This was consistent with previously observed solution pH values for cementation solutions with urea-to-calcium ratios of 1:1 following near full urea hydrolysis. In Column 3, however, initial pH values were significantly lower (near 6.8) due to limited generation of alkalinity from limited urea hydrolysis. As rinse injections proceeded, effluent pH values approached 7.0 for all columns after injecting 100 L. In all enriched columns (Column 1, 2, 4, 5), pH values then gradually increased to near steady values between 7.4 and 8.2 for the remainder of rinsing. The temporary reduction in outlet solution pH values was unexpected as the initial pH of the injected rinse solution was near 10. It is hypothesized that this pH reduction may have resulted from consumption of remaining carbonate species and some limited calcite precipitation upon the initial introduction of rinse solutions with 200 mM $Ca^{2+}$. Following the removal of sufficient solution alkalinity, increases in pH may then have occurred due to equilibration of high pH solutions with existing $CaCO_3$ and soil minerals. In Column 3, pH values remained lower than all enriched columns with final outlet well solution pH values near 6 to 6.5, which likely resulted from a lack of significant quantities of $CaCO_3$ minerals in this column.

Large reductions in effluent $NH_4^+$ from values between 497 mM and 524 mM (Column 1, 2, 4, 5) and $\approx 342$ mM (Column 3) to values between $\approx 20$ and 32 mM were observed in all columns at the outlet well after injecting 200 L (Fig. 4b). Following the application of an additional 200 L, however, $NH_4^+$ concentrations were only reduced to values between 3.5 and 9.0 mM. At the end of the 525 L injection, all effluent $NH_4^+$ concentrations were between 0.8 and 2.5 mM. It is hypothesized that the limited improvement in $NH_4^+$ removal after injecting significantly more rinse solution volume was influenced by soil-ion interactions and removal of sorbed $NH_4^+$ masses, though solution mixing via hydrodynamic dispersion may have also contributed. In order to evaluate the effect of these interactions on observed $NH_4^+$ trends, PHREEQC models were used to simulate passive tracer removal trends for all columns. As shown, concentrations were similar between measured $NH_4^+$ and modelled passive tracers early during rinsing due to limited breakthrough at the outlet well location, however, at injection volumes greater than 100 L, modeled passive tracer concentrations were significantly lower than experimentally observed $NH_4^+$ values. For example, reductions in passive ion concentrations to values below 10 mM required a maximum injection volume of 124 L for all models, however, physical experiments suggested that over twice that volume ($\approx 280$ L) was required to achieve these $NH_4^+$ levels. When integrating outlet well concentrations over injected volumes, measurements suggested the removal of 27.2, 27.2, 17.6, 38.6, and 28.2 moles of $NH_4^+$ occurred in Columns 1 through 5, respectively. This was equivalent to the removal of average pore fluid concentrations of 536 mM, 561 mM, 347 mM, 612 mM, and 560 mM $NH_4^+$ for Columns 1 through 5, respectively. Average pore fluid concentrations removed from Columns 1, 2, 4, and 5 exceeded the maximum expected $NH_4^+$ concentration of 500 mM and suggested that significant sorbed $NH_4^+$ masses must have been removed during rinsing.
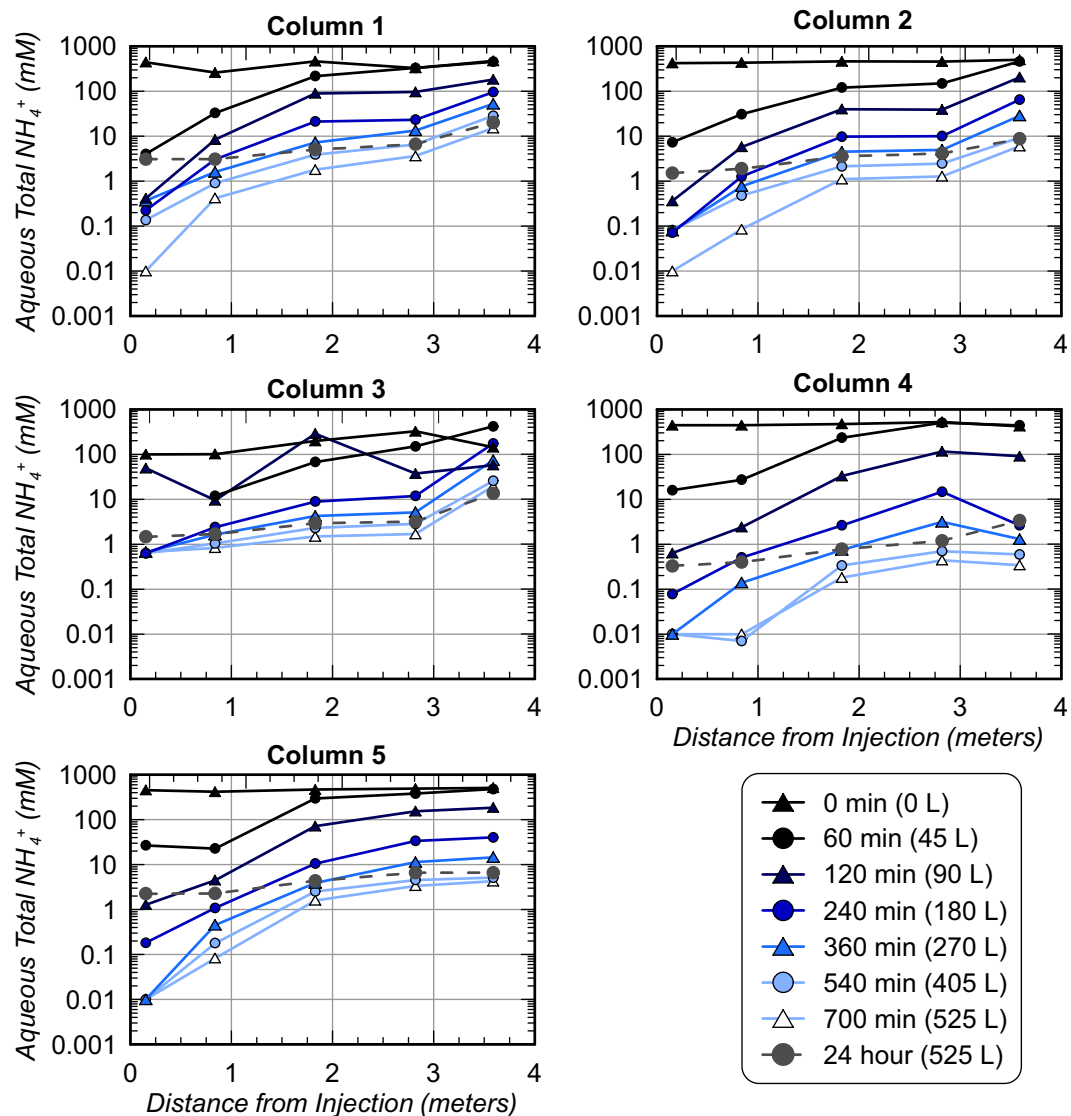
**Figure 5.** Contours of aqueous $NH_4^+$ concentrations within columns at all sampling port locations at various times during rinse injections. Measurement times after start of injections and cumulative injected rinse volumes are provided.

Retardation of $NH_4^+$ transport relative to passive ions was also previously observed in centimeter-scale experiments[25] and likely contributed to delayed $NH_4^+$ removal relative to passive tracer trends. Lastly, although $NH_4^+$ removal was expected to be reduced in Column 4 for similar rinse injection volumes due to a larger porosity, surprisingly, when injection volumes exceeded ≈200 L, an opposite trend was observed with much lower $NH_4^+$ concentrations exiting Column 4 compared to other columns. While unexpected, this was consistent with the greater $NH_4^+$ removal calculated for this column.

Figure 5 presents aqueous $NH_4^+$ concentrations measured spatially along soil columns at various points in time during rinse injections and 24 hours after rinse injections following a 12 hour stop flow period. Pre-rinsing measurements reflected conditions following the ninth cementation treatment, wherein most locations in enriched columns had $NH_4^+$ concentrations between ≈400 and 500 mM due to near full hydrolysis of the previously applied 250 mM urea injection. In Column 3, however, much lower $NH_4^+$ concentrations between 100 mM and 324 mM were observed and were consistent with the lower ureolytic activity observed in the augmented column during cementation treatments (Fig. 3). As rinse injections proceeded in time, significantly lower $NH_4^+$ concentrations were first observed at sampling locations closer to the injection well with large increases along column lengths. After injecting 45 L, almost no changes in $NH_4^+$ concentrations were observed near the outlet well (distance of 3.58 m), however, $NH_4^+$ concentrations were reduced to much lower values between 4 mM and 27 mM near the inlet well (distance of 0.15 m) in all columns. When comparing trends in time, spatial $NH_4^+$ concentrations were similar between Columns 1, 2, and 5, however, Column 3 and 4 trends were significantly different. Despite lower pre-treatment $NH_4^+$ concentrations in Column 3 prior to rinsing, trends in time were similar to other Concrete Sand columns when rinse volumes were less than ≈270 L. When additional rinse solution was
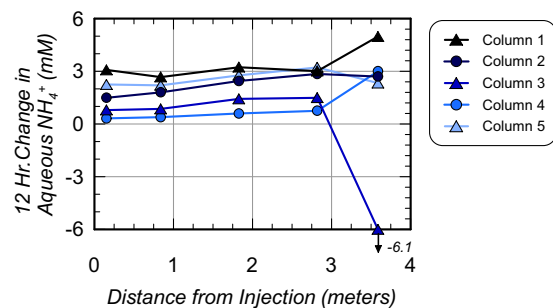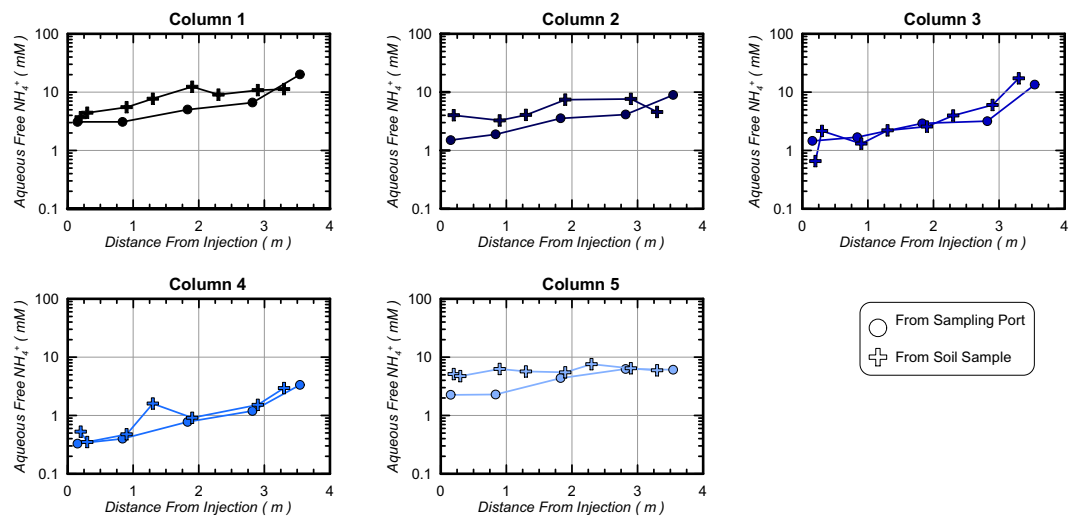
**Figure 6.** Changes in aqueous $NH_4^+$ concentrations following a 12 hour stop flow period after rinsing versus column length for all columns.
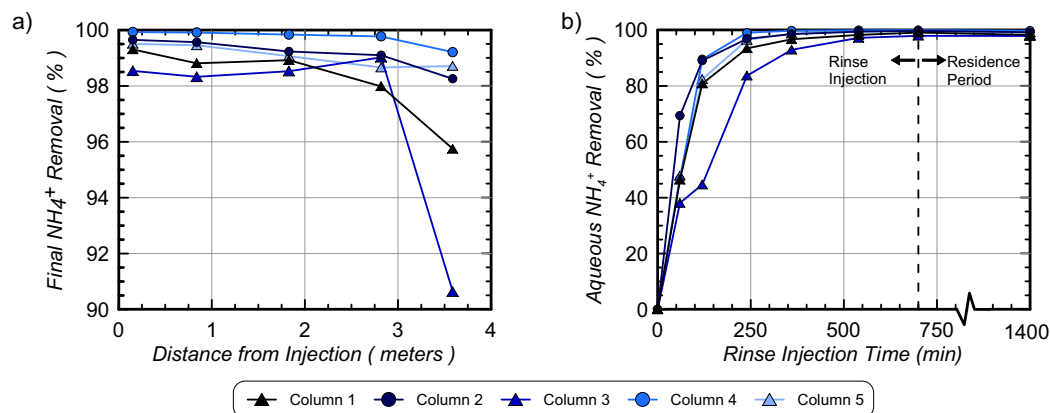


**Figure 7.** (**a**) Final $NH_4^+$ removal following the 12-hour stop flow period (in percent) versus column length and (**b**) cumulative $NH_4^+$ removal (in percent) versus rinse injection time.

applied to Column 3, however, continued reductions in $NH_4^+$ were not observed and most locations had concentrations exceeding 1 mM. Reduced $NH_4^+$ removal in Column 3 may have resulted from limited urea hydrolysis during the treatment period, the presence of more unoccupied cation exchange sites, and thus increased retardation of $NH_4^+$ transport. Additionally, lower pH values observed in this column during rinsing, may have resulted in more ammonium existing in the charged form $NH_4^+$ rather than $NH_3$. In Column 4, greater $NH_4^+$ removal was again observed for similar injection volumes, despite having a larger column pore volume. Higher exchangeable cation contents measured in Delta Sand may have prevented $NH_4^+$ from interacting with soil surfaces during rinsing, thus improving $NH_4^+$ removal efficiency. After injecting 525 L of rinse solutions, $NH_4^+$ concentrations were below 15 mM, 6 mM, 19 mM, 0.4 mM, and 4 mM at all locations in Columns 1 through 5, respectively. Following the 12 hour stop flow period, however, $NH_4^+$ concentrations generally increased and gradients in concentrations across columns became less pronounced likely due to equilibration of solutions with sorbed $NH_4^+$ concentrations and diffusion. Figure 6 presents changes in $NH_4^+$ concentrations during the stop flow period versus column length. Most locations had $NH_4^+$ increases between 1 and 5 mM during the stop flow period. Again, Column 1, 2, and 5 showed similar trends, with Column 3 and 4 differing. In Column 3, much smaller increases in $NH_4^+$ concentrations were observed with a single location achieving a 6.1 mM reduction during the retention period. Similarly, in Column 4, increases in concentrations were much lower than other columns and were generally near 0.3 mM. Smaller increases in $NH_4^+$ concentrations in these columns during the stop flow period may reflect more limited desorption of $NH_4^+$ resulting from less $NH_4^+$ exposure during treatments (Column 3) and saturation of sorption sites and limited $NH_4^+$ and soil interactions (Column 4).

Figure 7 presents (a) removal of pre-rinsing $NH_4^+$ concentrations (in percent) along column lengths and (b) cumulative $NH_4^+$ removal (in percent) for all columns in time. As shown in Fig. 7a, all locations achieved greater than 95.7% $NH_4^+$ removal following rinsing and the 12-hour residence period, with the exception of the most distal location in Column 3 (90.6% removal). At distances less than 2.82 m, greater removal was observed with all columns achieving greater than 98.0% $NH_4^+$ removal. Column 4 achieved the highest $NH_4^+$ removal of all columns with all locations achieving values above 99.2% removal. In order to better understand temporal changes in $NH_4^+$ removal, spatial contours of $NH_4^+$ at various times (Fig. 5) were integrated along column lengths to estimate cumulative $NH_4^+$ removal in time. As shown in Fig. 7b, all columns started with 0% removal before rinsing, and achieved between 38% and 69% $NH_4^+$ removal after injecting only 45 L (60 min). With increased rinse injection volumes, columns exhibited similar removal trends with the exception of Column 3, which achieved less removal in time. In all enriched columns, greater than 80% removal was achieved after injecting 90 L (120 min) and greater than 93% removal was achieved after injecting 180 L (240 min). Column 3, however, required near

**Figure 8.** Comparison of aqueous $NH_4^+$ concentrations between solution samples obtained from aqueous sampling ports (after the 12 hour stop flow period) and physical soil samples obtained post-rinsing.

270 L (360 min) to obtain 93% removal. Immediately following rinse injections, cumulative removal was 99.1%, 99.7%, 97.9%, 99.9%, and 99.6%, in Columns 1 through 5, respectively. However, after the stop flow period, removal percentages decreased by up to 0.9% and were 98.2%, 99.2%, 97.9%, 99.8%, and 99.1%, in Columns 1 through 5, respectively. Figure 8 presents $NH_4^+$ concentrations measured in aqueous solutions obtained from sampling ports after the stop flow period as well as solutions extracted from moist soil samples obtained post-rinsing at various locations. As shown, values obtained from both methods resulted in similar magnitudes and trends in $NH_4^+$ concentrations along columns suggesting that aqueous samples obtained from sampling ports were generally representative of internal soil conditions. $NH_4^+$ concentrations from soil samples, however, were consistently slightly higher than sampling port values suggesting that greater concentrations of $NH_4^+$ may have resided more locally around soil particle surfaces. Despite these differences, soil sample trends indicated post-rinsing $NH_4^+$ concentrations between 3.7 mM and 17 mM in Column 1, 2, 3, and 5 with greater removal and values between 0.3 mM and 2.9 mM in Column 4.

Figure 9a presents measurements of sorbed $NH_4^+$ masses as determined from KCl extracted soil versus free solution $NH_4^+$ measurements (Fig. 8). As shown, columns had measurable sorbed $NH_4^+$ masses that varied between $4.8 \times 10^{-4}$ and $3.6 \times 10^{-3}$ millimoles of $NH_4^+$ per gram of dry soil. In all columns, sorbed $NH_4^+$ masses increased with distance from the injection well location, suggesting reduced $NH_4^+$ removal from soil surfaces at larger distances. Figure 9b presents similar sorbed $NH_4^+$ masses as a percentage of soil cation exchange capacities. As shown, all sorbed $NH_4^+$ masses were between 1.9% and 16.1% of the total CEC of soil materials. Large differences were observed between soil types with Concrete Sand columns (Column 1, 2, 3) achieving average sorbed $NH_4^+$ masses of 5.8% CEC, Covelo Sand (Column 5) achieving the highest average sorbed $NH_4^+$ masses of 10.3% CEC, and Delta Sand (Column 4) achieving the lowest average sorbed $NH_4^+$ masses of 3.3% CEC. Figure 9c presents measurements of sorbed $NH_4^+$ masses with corresponding aqueous $NH_4^+$ concentrations obtained from soil samples. As expected, for all soil materials, when aqueous $NH_4^+$ concentrations were higher, sorbed $NH_4^+$ masses also increased. The apparent linear relationship between sorbed $NH_4^+$ masses and aqueous $NH_4^+$ concentrations in equilibrium with soil surfaces suggested that $NH_4^+$ sorption in columns may be reasonably described by a Freundlich adsorption isotherm over the concentrations observed[41]. Linear relationships between free $NH_4^+$ concentrations and sorbed $NH_4^+$ masses have been similarly observed in other studies examining ammonium sorption kinetics in soils[42,43]. Furthermore, this correlation suggests that sorbed $NH_4^+$ concentrations were likely higher prior to rinsing and were reduced during the rinsing process. This is consistent with the higher removed $NH_4^+$ concentrations estimated from outlet well measurements (Fig. 4). In order to better understand the amount of $NH_4^+$ remaining on soil particle surfaces, "effective" aqueous $NH_4^+$ concentrations were calculated assuming that all sorbed $NH_4^+$ was instead available to surrounding aqueous solutions. Figure 9d presents "effective" $NH_4^+$ concentrations with distance along all columns computed from known column pore volumes and soil masses. As shown, effective $NH_4^+$ concentrations ranged between 5.6 mM and 56.6 mM for all columns. This suggested that if sorbed $NH_4^+$ masses entered into free solution, aqueous $NH_4^+$ concentrations would increase by 0.05 mM to 42.8 mM. Again, the highest effective $NH_4^+$ concentrations were calculated for Column 3 and the lowest effective $NH_4^+$ concentrations were in Column 4. While these $NH_4^+$ ions remained sorbed to soils under conditions present during the stop flow period, sorbed $NH_4^+$ may present challenges related to desorption over time as groundwater solutions are transported through treated locations.

Figure 10 presents contours of soil $V_s$ measured along columns lengths for all columns before cementation injections, after cementation but before rinsing, and after rinsing injections following the stop flow period. All columns had similar initial $V_s$ values, however, after cementation treatments, large differences in $V_s$ distributions were observed between columns and were reflective of differences in bio-cementation distributions. In Column 1, which had the highest ureolytic activity, high magnitudes of cementation were observed at distances less than 2.35 m with $V_s$ values

11
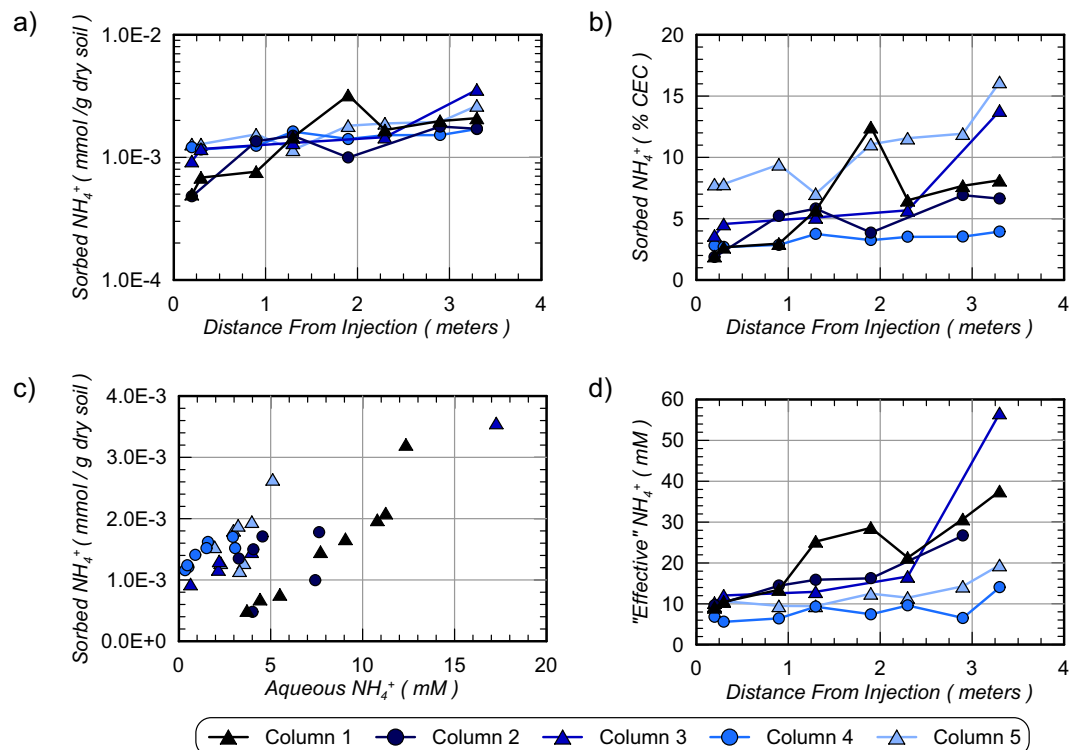
**Figure 9.** (**a**) Sorbed $NH_4^+$ masses versus column lengths, (**b**) sorbed $NH_4^+$ masses as a percentage of soil CEC versus column lengths, (**c**) sorbed $NH_4^+$ masses versus aqueous $NH_4^+$ concentrations, and (**d**) "effective" aqueous $NH_4^+$ concentrations versus column lengths.

ranging from 1107 m/s to 1522 m/s with a large reduction in $V_s$ to 382 m/s at a distance of 3.37 m. In Column 2, which contained the same sand but had a lower ureolytic activity, $V_s$ values ranged between 723 m/s and 1186 m/s at distances less than 2.35 m, however, a $V_s$ of 546 m/s was obtained at 3.37 m, which was significantly greater than Column 1. In Column 3, which was augmented, a $V_s$ of 1197 m/s was obtained near the injection well, however, little cementation was detected at distances greater than 0.31 m. In Column 4 and 5, which had lower ureolytic activity, similar trends were observed along column lengths as Column 2, with slightly lower $V_s$ values between 817 m/s and 871 m/s measured at a distance of 0.31 m and values between 227 m/s and 401 m/s measured at a distance of 3.37 m. For all columns, $V_s$ values before and after rinsing differed by no more than ± 50 m/s suggesting that little dissolution or precipitation had occurred. To further examine trends during rinsing, changes in $V_s$ values were plotted in time during rinse injections for all columns and bender element locations (Fig. 11). No consistent trends between columns or measurement locations were observed. Immediately after the start of injections, locations had changes in $V_s$ values between −46 m/s and +14 m/s, however, following the stop flow period changes between −33 m/s and +43 m/s were observed. These $V_s$ results suggest that rinse injections likely only resulted in minor changes in calcite contents between −0.2% and +0.3% by mass following previous relationships established by Gomez and DeJong (2017)[7].

## Conclusions

The production of $NH_4^+$ by-products during ureolytic bio-cementation presents a significant challenge for the technology, which must be addressed if MICP is to attain widespread acceptance as an environmentally-conscious ground improvement alternative. In this study, five 3.7-meter long soil columns containing three different sandy soils were treated using different bio-cementation treatment techniques to investigate $NH_4^+$ by-product removal following ureolytic bio-cementation. During treatments, differences in enriched and augmented ureolytic activity were achieved and resulted in differences in bio-cementation distributions. While all enriched columns achieved near full hydrolysis of applied 250 mM urea injections over 24 hours (Column 1) and 48 hours (Column 2, 4, 5), the augmented Column 3 achieved limited urea hydrolysis and less $NH_4^+$ production during cementation treatments. The localization of ureolytic activity and cementation observed near the injection well in Column 3 was attributed to the filtration of *S. pasteurii* bacterial cells during augmentation. Following cementation, a single 525 L volume of a high pH and high ionic strength rinse solution (200 mM $CaCl_2$, pH ≈10.0) was applied to each column and $NH_4^+$ removal and cementation integrity were monitored. $NH_4^+$ concentrations observed at the outlet well were compared to expected trends for a passive tracer and results suggest that $NH_4^+$ transport was retarded by soil-ion interactions with significantly greater $NH_4^+$ removal than expected due to removal of sorbed $NH_4^+$ from soil surfaces. When spatial changes in $NH_4^+$ concentrations were examined during rinsing, large gradients in $NH_4^+$ concentrations were observed across columns, however, $NH_4^+$ concentrations below 19 mM were observed at all locations immediately after rinsing. After a 12-hour stop flow period, increases in $NH_4^+$ concentrations between 1 and 5 mM at most locations were observed, with final cumulative $NH_4^+$ removal between 97.9% and 99.8%, achieved for all columns.
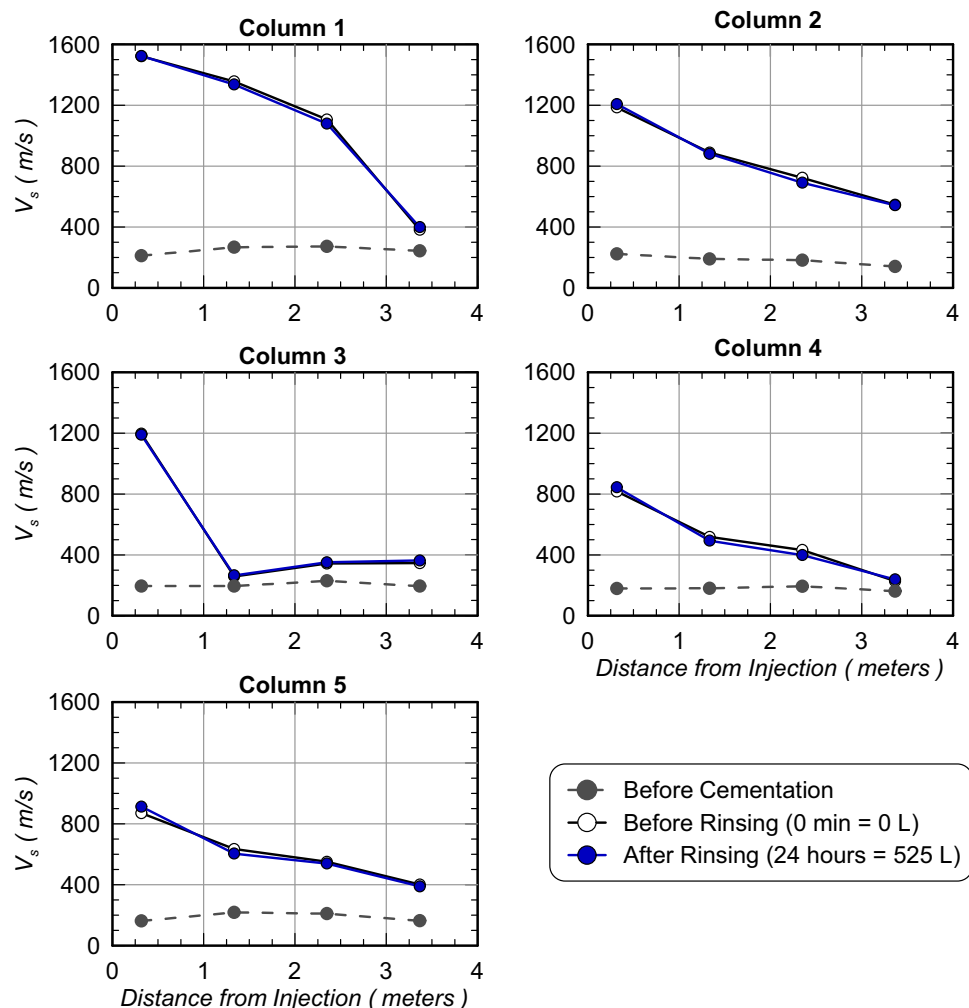
**Figure 10.** Soil shear wave velocities ($V_s$) versus column lengths for all columns before cementation, after cementation and immediately before rinsing, and after rinsing.
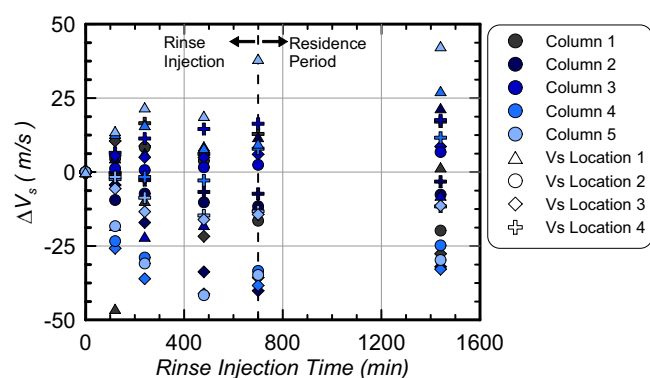


**Figure 11.** Changes in soil shear wave velocities ($V_s$) for all bender element sensor locations in all columns versus time since the start of rinsing injections.

Greater $NH_4^+$ removal observed in Column 4 was attributed to higher concentrations of exchangeable cations present in the marine soil, which may have limited interactions between $NH_4^+$ and soil minerals. In contrast, limited $NH_4^+$ removal observed in Column 3 was believed to have resulted from both the presence of more unoccupied sorption sites from limited urea hydrolysis and lower pH values observed during rinsing. Following KCl extraction of post-rinsing soil samples, measurements suggested that significant $NH_4^+$ remained sorbed to soil surfaces, which

may present challenges related to $NH_4^+$ desorption over time. Finally, soil $V_s$ measurements suggested that $NH_4^+$ removal had no significant effect on cementation integrity. While these results suggest that $NH_4^+$ can be successfully removed from aqueous solutions residing in bio-cemented soils, acceptable limits for aqueous $NH_4^+$ concentrations and sorbed $NH_4^+$ masses will likely be governed by site-specific requirements and may require further investigation of rinsing and management techniques.

## Data availability

The datasets generated during and/or analyzed during the current study are available from the corresponding author on reasonable request. All measured data presented in the figures of this paper will be available through the NSF DesignSafe-CI Data Depot repository (https://www.designsafe-ci.org/data/browser/public/) under project number PRJ-2467.

## References

1. DeJong, J. T. *et al*. Biogeochemical processes and geotechnical applications: progress, opportunities and challenges. *Géotechnique* **63**(4), 287 (2013).
2. Seagren, E.A., & Aydilek, A.H. Biomediated geomechanical processes. *Environmental Microbiology*, 2nd Ed., 319–348 (2010).
3. El Mountassir, G., Minto, J. M., van Paassen, L. A., Salifu, E. & Lunn, R. J. Applications of microbial processes in geotechnical engineering. In *Advances in applied microbiology* (Vol. 104, pp. 39-91). Academic Press. (2018).
4. Stocks-Fisher, S., Galinat, J. K. & Bang, S. S. Microbiological precipitation of CaCO3. *Soil Biology and Biochemistry* **31**(11), 1563–1571 (1999).
5. DeJong, J., Fritzges, M. & Nüsslein, K. Microbial induced cementation to control sand response to undrained shear. *Journal of Geotechnical and Geoenvironmental Engineering* **132**(11), 1381–1392 (2006).
6. Gomez, M. G., DeJong, J. T. & Anderson, C. M. Effect of Bio-cementation on Geophysical and Cone Penetration Measurements in Sands. *Canadian Geotechnical Journal* **55**(11), 1632–1646 (2018).
7. Gomez, M. G., & DeJong, J. T. Engineering Properties of Bio-Cementation Improved Sandy Soils. *Grouting 2017 Technical Papers*, ASCE, Reston, VA, 23–33 (2017).
8. Montoya, B. M. & DeJong, J. T. Stress-strain behavior of sands cemented by microbially induced calcite precipitation. *Journal of Geotechnical and Geoenviron. Engineering* **141**(6), 04015019 (2015).
9. Fujita, Y. *et al*. Strontium incorporation into calcite generated by bacterial ureolysis. *Geochimica et Cosmochimica Acta* **68**(15), 3261–3270 (2004).
10. Montoya, B. M., DeJong, J. T. & Boulanger, R. W. Dynamic response of liquefiable sand improved by microbial-induced calcite precipitation. *Géotechnique* **63**(4), 302–312 (2013).
11. Minto, J. M., MacLachlan, E., El Mountassir, G. & Lunn, R. J. Rock fracture grouting with microbially induced carbonate precipitation. *Water Resources Research* **52**(11), 8827–8844 (2016).
12. Phillips, A. J. *et al*. Fracture sealing with microbially-induced calcium carbonate precipitation: A field study. *Environmental Science & Technology* **50**(7), 4111–4117 (2016).
13. O'Donnell, S. T., Rittmann, B. E. & Kavazanjian, E. Jr. MIDP: Liquefaction mitigation via microbial denitrification as a two-stage process. I: Desaturation. *Journal of Geotechnical and Geoenvironmental Engineering* **143**(12), 04017094 (2017).
14. Gomez, M. G., Graddy, C. M., DeJong, J. T., Nelson, D. C. & Tsesarsky, M. Stimulation of Native Microorganisms for Biocementation in Samples Recovered from Field-Scale Treatment Depths. *Journal of Geotechnical and Geoenvironmental Engineering* **144**(1), 04017098 (2018).
15. van Paassen, L. A. Bio-mediated ground improvement: from laboratory experiment to pilot applications. *Geo-Frontiers 2011 Technical Papers*, ASCE, Reston, VA, 4099–4108 (2011).
16. Smith R. W., Fujita Y., Hubbard S. S. & Ginn T. R. US Department of Energy Final Report Grant No. DE-FG02– 07ER64404: Field Investigations of Microbially Facilitated Calcite Precipitation for Immobilization of Strontium-90 and other Trace Metals in the Subsurface. US Department of Energy, Washington, DC, pp. 1–20, Technical Report DEO/ ER64404-01. (2012).
17. Gomez, M. G. *et al*. Field-scale bio-cementation tests to improve sands. *Proceedings of the Institution of Civil Engineers-Ground Improvement* **168**(3), 206–216 (2015).
18. Gomez, M. G. *et al*. Large- scale comparison of bioaugmentation and biostimulation approaches for biocementation of sands. *Journal of Geotechnical and Geoenvironmental Engineering* **143**(5), 04016124 (2017).
19. Saneiyan, S. *et al*. Induced polarization as a monitoring tool for *in-situ* microbial induced carbonate precipitation (MICP) processes. *Ecological Engineering* **127**, 36–47 (2019).
20. Zamani, A. & Montoya, B. M. Undrained cyclic response of silty sands improved by microbial induced calcium carbonate precipitation. *Soil Dynamics and Earthquake Engineering* **120**, 436–448 (2019).
21. Gat, D., Ronen, Z. & Tsesarsky, M. Long-term sustainability of microbial-induced CaCO3 precipitation in aqueous media. *Chemosphere* **184**, 524–531 (2017).
22. Paerl, H. W. Coastal eutrophication and harmful algal blooms: Importance of atmospheric deposition and groundwater as "new" nitrogen and other nutrient sources. *Limnology and Oceanography,* **42**(5part2), 1154–1165 (1997).
23. U.S. Environmental Protection Agency. *Aquatic Life Ambient Water Quality Criteria for Ammonia – Freshwater* (EPA Publication No. 822-R-13-001). Washington, DC, 1–255 (2013).
24. Cuthbert, M. O. *et al*. A field and modeling study of fractured rock permeability reduction using microbially induced calcite precipitation. *Environmental Science & Technology* **47**(23), 13637–13643 (2013).
25. Lee, M., Kolbus, C. M., Yepez, A. D., & Gomez, M. G. Investigating Ammonium By-Product Removal following Stimulated Ureolytic Microbially-Induced Calcite Precipitation. In *Geo-Congress 2019: Soil Improvement* (pp. 260–272). Reston, VA: American Society of Civil Engineers (2019).
26. San Pablo, A. C. *et al*. Meter-scale Bio-cementation Experiments to Advance Process Control and Reduce Impacts: Examining Spatial Control, Ammonium By-product Removal, and Chemical Reductions. *Journal of Geotechnical and Geoenvironmental Engineering*. Under Review (2019).
27. Gomez, M. G., Anderson, C. M., DeJong, J. T., Nelson, D. C. & Lau, X. Stimulating *in situ* soil bacteria for bio-cementation of sands. *Geo-Congress 2014 Technical Papers*, ASCE, Reston, VA. 1674−1682 (2014).
28. Graddy, C. M. *et al*. Diversity of Sporosarcina-like Bacterial Strains Obtained from Meter-Scale Augmented and Stimulated Biocementation Experiments. *Environmental Science & Technology* **52**(7), 3997–4005 (2018).
29. "Standard Practice for Classification of Soils for Engineering Purposes (Unified Soil Classification System)." *ASTM International*. West Conshohocken, PA (2010).

30. Ferris, F. G., Phoenix, V., Fujita, Y. & Smith, R. W. Kinetics of calcite precipitation induced by ureolytic bacteria at 10 to 20 °C in artificial groundwater. *Geochim. Cosmochim. Acta.* **68**(8), 1701–1722 (2004).
31. Parkhurst, D. L. & Appelo, C. A. J. Description of input and examples for PHREEQC version 3–A computer program for speciation, batch-reaction, one-dimensional transport, and inverse geochemical calculations. *U.S. Geological Survey Techniques and Methods*, book 6, chap. A43, 497 p. (2013).
32. Krom, M. D. Spectrophotometric determination of ammonia: a study of a modified Berthelot reaction using salicylate and dichloroisocyanurate. *Analyst* **105**(1249), 305–316 (1980).
33. Knorst, M. T., Neubert, R. & Wohlrab, W. Analytical methods for measuring urea in pharmaceutical formulations. *J. Pharm. Biomed. Anal.* **15**(11), 1627–1632 (1997).
34. Hobbie, J. E., Daley, R. J. & Jasper, S. Use of Nuclepore filters for counting bacteria by fluorescence microscopy. *Applied Environmental Microbiology.* **33**(5), 1225–1228 (1977).
35. U.S. Environmental Protection Agency. *Cation-exchange capacity of soils (ammonium acetate): test methods for evaluating solid waste.* SW846, method 9080. Washington, DC: USEPA, Office of Solid Waste and Emergency Response (1986).
36. Keeney, D. R. & Nelson, D. W. Nitrogen—Inorganic Forms 1. *Methods of soil analysis. Part 2. Chemical and microbiological properties*, pp. 643-698 (1982).
37. Mengel, D. B.. Fundamentals of soil cation exchange capacity (CEC). Purdue Univ. Coop. Ext. Ser. AY-238. 2 p. (1980).
38. Brusseau, M. L. The influence of solute size, pore water velocity, and intraparticle porosity on solute dispersion and transport in soil. *Water Resources Research* **29**(4), 1071–1080 (1993).
39. van Paassen, L. A., Ghose, R., van der Linden, T. J. M., van der Star, W. R. L. & van Loosdrecht, M. C. M. Quantifying Bio-Mediated Ground Improvement by Ureolysis: A Large Scale Biogrout Experiment. *Journal of Geotechnical and Geoenvironmental Engineering* **1**(1), 237–237 (2010).
40. Ginn, T. R. *et al*. Processes in microbial transport in the natural subsurface. *Advances in Water Resources* **25**(8–12), 1017–1042 (2002).
41. Freundlich, H. Über die adsorption in lösungen. *Zeitschrift für physikalische Chemie* **57**(1), 385–470. (1907).
42. Huang, H., Xiao, X., Yan, B. & Yang, L. Ammonium removal from aqueous solutions by using natural Chinese (Chende) zeolite as adsorbent. *Journal of Hazardous materials* **175**(1–3), 247–252 (2010).
43. Uğurlu, M. & Karaoğlu, M. H. Adsorption of ammonium from an aqueous solution by fly ash and sepiolite: isotherm, kinetic and thermodynamic analysis. *Microporous and Mesoporous Materials* **139**(1–3), 173–178 (2011).

## Acknowledgements

## Author contributions

Minyong Lee was involved in the design, performance, and analysis of data obtained from the presented experiments, and co-wrote the first draft of the main manuscript text and prepared figures. Michael G. Gomez was involved in the design, performance, and analysis of data obtained from the presented experiments, and co-wrote the first draft of the main manuscript text and prepared figures. Colin M. Kolbus was involved in the design, performance, and analysis of data obtained from the presented experiments and reviewed and contributed to the final manuscript. Alexandra C.M. San Pablo was involved in the design, performance, and analysis of data obtained from the presented experiments and reviewed and contributed to the final manuscript. Charles M.R. Graddy was involved in the design, performance, and analysis of data obtained from the presented experiments and reviewed and contributed to the final manuscript. Jason T. DeJong was involved in the design, performance, and analysis of data obtained from the presented experiments and reviewed and contributed to the final manuscript. Douglas C. Nelson was involved in the design, performance, and analysis of data obtained from the presented experiments and reviewed and contributed to the final manuscript.

## Competing interests

The authors declare no competing interests.

## Additional information

**Correspondence** and requests for materials should be addressed to M.G.G.

**Reprints and permissions information** is available at www.nature.com/reprints.

**Publisher's note** Springer Nature remains neutral with regard to jurisdictional claims in published maps and institutional affiliations.